Atmos. Meas. Tech., 9, 4029–4049, 2016
www.atmos-meas-tech.net/9/4029/2016/
doi:10.5194/amt-9-4029-2016

Atmospheric Measurement Techniques
Open Access
EGU

Proposed standardized definitions for vertical resolution and uncertainty in the NDACC lidar ozone and temperature algorithms – Part 1: Vertical resolution

Thierry Leblanc[1], Robert J. Sica[2], Joanna A. E. van Gijsel[3], Sophie Godin-Beekmann[4], Alexander Haefele[5], Thomas Trickl[6], Guillaume Payen[7], and Frank Gabarrot[7]

[1]Jet Propulsion Laboratory, California Institute of Technology, Wrightwood, CA 92397, USA
[2]Department of Physics and Astronomy, The University of Western Ontario, London, Canada
[3]Royal Netherlands Meteorological Institute (KNMI), Bilthoven, the Netherlands
[4]LATMOS-IPSL, CNRS-INSU, Paris, France
[5]Meteoswiss, Payerne, Switzerland
[6]Karlsruher Institut für Technologie, IMK-IFU, Garmisch-Partenkirchen, Germany
[7]Observatoire des Sciences de l'Univers de La Réunion, CNRS and Université de la Réunion (UMS3365), Saint Denis de la Réunion, France

Correspondence to: Thierry Leblanc (thierry.leblanc@jpl.nasa.gov)

Received: 6 April 2016 – Published in Atmos. Meas. Tech. Discuss.: 25 April 2016
Revised: 22 July 2016 – Accepted: 27 July 2016 – Published: 25 August 2016

Abstract. A standardized approach for the definition and reporting of vertical resolution of the ozone and temperature lidar profiles contributing to the Network for the Detection for Atmospheric Composition Change (NDACC) database is proposed. Two standardized definitions homogeneously and unequivocally describing the impact of vertical filtering are recommended.

The first proposed definition is based on the width of the response to a finite-impulse-type perturbation. The response is computed by convolving the filter coefficients with an impulse function, namely, a Kronecker delta function for smoothing filters, and a Heaviside step function for derivative filters. Once the response has been computed, the proposed standardized definition of vertical resolution is given by $\Delta z = \delta z \times H_{\mathrm{FWHM}}$, where δz is the lidar's sampling resolution and H_{FWHM} is the full width at half maximum (FWHM) of the response, measured in sampling intervals.

The second proposed definition relates to digital filtering theory. After applying a Laplace transform to a set of filter coefficients, the filter's gain characterizing the effect of the filter on the signal in the frequency domain is computed, from which the cut-off frequency f_{C}, defined as the frequency at which the gain equals 0.5, is computed. Vertical resolution is then defined by $\Delta z = \delta z/(2 f_{\mathrm{C}})$. Unlike common practice in the field of spectral analysis, a factor $2 f_{\mathrm{C}}$ instead of f_{C} is used here to yield vertical resolution values nearly equal to the values obtained with the impulse response definition using the same filter coefficients. When using either of the proposed definitions, unsmoothed signals yield the best possible vertical resolution $\Delta z = \delta z$ (one sampling bin).

Numerical tools were developed to support the implementation of these definitions across all NDACC lidar groups. The tools consist of ready-to-use "plug-in" routines written in several programming languages that can be inserted into any lidar data processing software and called each time a filtering operation occurs in the data processing chain.

When data processing implies multiple smoothing operations, the filtering information is analytically propagated through the multiple calls to the routines in order for the standardized values of vertical resolution to remain theoretically and numerically exact at the very end of data processing.

Published by Copernicus Publications on behalf of the European Geosciences Union.

1 Introduction

As part of the Network for the Detection of Atmospheric Composition Change (NDACC, website: http://www.ndsc.ncep.noaa.gov/), over 20 ground-based lidar instruments are dedicated to the long-term monitoring of atmospheric composition and to the validation of space-borne measurements of Earth's atmosphere from environmental satellites (e.g., EOS-Aura, ENVISAT, NPP, the Sentinels). In networks such as NDACC, the instruments use a wide spectrum of methodologies and technologies to measure key atmospheric parameters such as ozone, temperature, and water vapor. One ensuing caveat is the difficulty of archiving measurement and analysis information consistently within such a varied ensemble of passive and active remote-sensing instruments; yet the need for consistent definitions has strengthened as datasets of various origins (e.g., satellite and ground-based) need higher quality control and thorough validation before they can be used for long-term trend studies or be assimilated into global systems. For example, recommendations were recently made for the use of specific effective vertical resolution schemes within the European Aerosol Research Lidar Network (EARLINET; Iarlori et al., 2015), and efforts were made to produce aerosol lidar retrievals with a prescribed level of standardization (D'Amico et al., 2015). Within the NDACC lidar working group, a few studies have shown the impact on ozone concentration and uncertainty of using different definitions of vertical resolution (e.g., Beyerle and McDermid, 1999; Godin et al., 1999), or have estimated the impact of various corrections on temperature (e.g., Leblanc et al., 1998), but little work has been done to facilitate a standardization of the definitions and approaches relating to vertical resolution and uncertainty budget in NDACC lidar retrievals.

To address these and other lidar retrieval issues, a group of lidar experts formed an International Space Science Institute team of experts in 2011 (http://www.issibern.ch/aboutissi/mission.html). The objective of this working group (henceforth the ISSI team) was to provide scientifically meaningful recommendations for the use of standardized definitions of vertical resolution and standardized definitions and approaches for the treatment of uncertainty in the NDACC ozone and temperature lidar retrievals. Ultimately, the recommendations compiled in an ISSI team report (Leblanc et al., 2016a) were designed to be implemented consistently by all NDACC ozone and temperature lidar investigators.

The present article is the first of three companion papers that provide a comprehensive description of the recommendations made by the ISSI team to the NDACC lidar community for the standardization of vertical resolution and uncertainty. The present article (Part 1) is exclusively dedicated to the description of the proposed standardized vertical resolution. A second paper (Part 2) (Leblanc et al., 2016b) reviews the proposed standardized definitions and approaches for the ozone differential absorption lidars' uncertainty budget. The last paper (Part 3) (Leblanc et al., 2016c) reviews the proposed standardized definitions and approaches for the NDACC temperature lidars' uncertainty budget. Details that appear beyond the scope of the present three companion papers may be found in the ISSI team report (Leblanc et al., 2016a).

Though the ISSI team focus has been on the retrieval of ozone using the differential absorption technique (Mégie et al., 1977), and the retrieval of temperature using the density integration technique (Hauchecorne and Chanin, 1980; Arshinov et al., 1983), most recommendations made in the present and two companion papers can be followed for the retrieval of other NDACC lidar species such as water vapor (Raman and differential absorption techniques), temperature (rotational Raman technique), and aerosol backscatter ratio. One exception is when using an optimal estimation method (OEM) for the retrieval of temperature or water vapor mixing ratio as recently proposed by Sica and Haefele (2015, 2016), for which vertical resolution is implicitly determined from the full width at half maximum of the OEM's averaging kernels.

Vertical resolution, as provided in the lidar data files, is an indicator of the amount of vertical filtering applied to the lidar signals or to the measured species profiles. This filtering is applied in order to reduce high-frequency noise typically produced at the signal detection level. A higher vertical resolution means that the instruments are able to detect features of small vertical extent, while a lower vertical resolution implies a reduced ability to detect features of small vertical scale. Typically, vertical resolution is provided in a unit of vertical length (e.g., meter). Because the lidar signal-to-noise ratio strongly varies with altitude, the amount of filtering typically applied also varies with altitude, with more filtering applied at higher altitude ranges unless specific geophysical processes are investigated (e.g., gravity waves, stratospheric intrusions).

Here the word "filtering" is preferred to the word "smoothing" because it is more general and applies to both smoothing and differentiation processes, the former process being relevant to both temperature and ozone lidar retrievals, and the latter process being relevant to the ozone differential absorption technique. To optimize the useful range of lidar measurements, most lidar signals or profiles are digitally filtered at some point in the retrieval process. Over the years, NDACC lidar investigators have provided temperature and ozone profiles using a wide range of vertical resolution schemes and values, where the definition of vertical resolution appears to differ significantly. The objective of the present work is not to recommend a specific vertical resolution scheme, but instead to ensure that the definition used by the data providers to describe their scheme is reported and interpreted consistently across the entire network. The approaches and recommendations in this article were designed so that they can be implemented consistently by all NDACC lidar investigators and beyond (e.g., the Tropospheric Ozone Lidar

Network, TOLNet, website: http://www-air.larc.nasa.gov/missions/TOLNet/, or the GCOS Reference Upper Air Network, GRUAN, website: http://www.dwd.de/EN/research/international-programme/gruan/home.html). We therefore recommend two well-known definitions, one definition based on the full width at half maximum (FWHM) of a finite impulse response, and the other definition based on the cut-off frequency of digital filters. These definitions allow a clear mapping of the amount of filtering applied to the lidar signal or species profile with the values of vertical resolution actually reported in the data files.

Section 2 summarizes the basics of digital signal filtering, and provides a few examples of how vertical resolution can be expressed in terms of impulse response and digital filter cut-off frequency. Section 3 reviews a number of vertical resolution definitions used by the NDACC ozone and temperature lidar community. The results from Sects. 2 and 3 are used in Sect. 4 to recommend and detail two practical, well-known definitions of vertical resolution that can be easily linked to the underlying filtering processes. The numerical values of vertical resolution computed using these two definitions are compared for several types of digital filters. For the sake of completeness, a Supplement to the present paper provides additional characteristics of several commonly used smoothing and derivative filters.

Numerical tools were developed by the ISSI team to facilitate the implementation of the proposed standardized definitions. The tools consist of subroutines written in four scientific programming languages (IDL, MATLAB, FORTRAN, and Python) that can be inserted in the lidar investigators' data processing software in order to compute the numerical values of the standardized vertical resolution. The plug-in routines are available upon request from the corresponding author.

2 Brief review of signal filtering theory

In this section we briefly review the mathematical background that allows us to link vertical resolution to the lidar signal (or profile) filtering process. Signal filtering for lidar data processing consists of either smoothing, differentiating or smoothing, and differentiating at the same time. To describe the filtering process, a signal S is defined in its general sense; i.e., it can be either a raw lidar signal from a single detection channel, the ratio of the corrected signals from two detection channels, or an unsmoothed ozone profile, temperature profile, calibrated or uncalibrated water vapor profile, etc. The only common requirement is that the signal is formed of a finite number of equally spaced samples in the vertical dimension $S(k)$ with $k = [1, nk]$. The constant interval between two samples, $\delta z = z(k+1) - z(k)$ for all k, is the sampling width, or sampling resolution, and corresponds to the smallest vertical interval that can be resolved by the lidar instrument.

The signal filtering process at an altitude $z(k)$ consists of convolving a set of $2N+1$ coefficients c_n with the signal S over the interval $\Delta z = 2N\delta z$ of boundaries $z(k-N)$ and $z(k+N)$ (e.g., Hamming, 1989):

$$S_{\mathrm{f}}(k) = \sum_{n=-N}^{N} c_n S(k+n), \tag{1}$$

where S_{f} is the signal after filtering. The transformation associated with this process is known as a non-recursive digital filter and is the simplest kind of digital filter. The elements of the vector, c_n, are the coefficients of the filter. A simple example of this type of filter is the arithmetic average for which all coefficients take the same value $c_n = 1/(2N+1)$. Several other filter names exist for this particular example, for example, boxcar smoothing filter, boxcar function, or smoothing by $[2N+1]$s (Hamming, 1989).

The number of filter coefficients and the values of these coefficients determine the actual effect of the filter on the signal. Three critical aspects of the effect of the filter on the signal are (1) the amount of noise reduction due to filtering, (2) the nature and degree of symmetry/asymmetry of the coefficients around the central value which determines whether the filter's function is to smooth, sum, differentiate, or interpolate, and (3) whether the magnitude of specific noise frequencies are being amplified or reduced after filtering. In the particular case of an unfiltered signal comprised of independent samples, and assuming that the variance of the noise for the unfiltered signal is constant through the filtering interval considered ($\sigma_S^2(k') = \sigma^2$ for all k' in the interval $[k-N, k+N]$), we obtain a simple relation that estimates the variance of the output signal:

$$\sigma_{S_{\mathrm{f}}}{}^2(k) = \sigma_{\mathrm{S}}^2 \sum_{n=-N}^{N} c_n^2. \tag{2}$$

This relation reveals the importance of the sum of the squared coefficients to determine the amount of noise reduction. However, it does not provide any information on the ability of the filter to distinguish what is noise and what is actual signal. To illustrate this problem, Fig. 1 shows an example of a noisy signal before and after filtering, processed using two different filters. We start from a modeled signal represented by the green dash-dotted curve. To this ideal signal, we add random noise, whose amplitude is distributed following Poisson statistics (signal detection noise). The noisy unfiltered signal is represented in this figure by a dark gray dotted curve. The signal is then processed using two different filters, i.e., two different sets of coefficients. The blue curve shows the filtered signal using least-squares linear fitting (identical to boxcar average, labeled LS-1), while the red curve shows the filtered signal, this time using least-squares fitting with a polynomial of degree 2 (LS-2). The number of terms used by both filters is the same ($2N+1 = 11$). The values of the coefficients, and not the number of coefficients, are responsible for the observed performance trade-off, here the trade-off

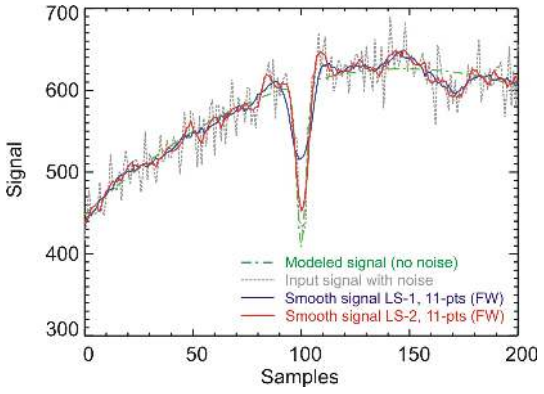

Figure 1. Example of the differing impact of two smoothing filters of identical number of terms ($2N+1=11$). The green dash-dotted curve is the modeled signal (with no noise), the gray dotted curve is the modeled input signal containing Poisson noise, the blue and red curves are the smoothed signal using an 11-point boxcar average (LS-1), and the least-squares fitting method with a polynomial of degree 2 (LS-2), respectively.

between a smoother signal and a noisier signal where the dip in the measurements is better reproduced.

In the real world, we typically do not know the exact nature or behavior of the measured signal. Consider the example in Fig. 1: if the definition used to report vertical resolution in the data files were based on the number of points used by the filter, we would not be able to attribute the differences observed between the blue and red curves to a difference in the filtering procedure. We therefore need to find some analytical way to characterize a specific filter if we want to understand its exact effect on the signal and properly interpret features observed on the smoothed signal. We will see thereafter that it is indeed possible to determine the resolution of the filter by either quantifying the response of a controlled impulse in the physical domain, or by using a frequency approach and studying the frequency response of the filter.

2.1 Classical approach: unit impulse response and unit step response

The impact of a specific filter on the signal can be characterized by computing the unit impulse response in the physical domain (usually called the time domain in time series analysis). This can be done by using a well-known, controlled input signal, e.g., an impulse, and by studying its response after being convolved by the filter coefficients. Considering a finite impulse response is equivalent to considering the output signal I_{OUT} formed by the convolution of an impulse I_{INP} with a finite number of coefficients c_n:

$$I_{\mathrm{OUT}}(k) = \sum_{n=-N}^{N} c_n I_{\mathrm{INP}}(k+n). \quad (3)$$

For smoothing non-derivative filters, this impulse is the discrete Kronecker delta function δ_{k0} (also called unit impulse function), which takes a value of 1 at coordinate $k=k_0$ and 0 elsewhere:

$$\delta_{k0}(k) = 1 \quad \text{for} \quad k = k_0$$
$$\delta_{k0}(k) = 0 \quad \text{for all} \quad k \neq k_0. \quad (4)$$

Using our smoothing interval of $2N+1$ points centered at altitude $z(k)$, the input impulse for which the response is needed will have a value of 1 at the central point, and 0 at all other points:

$$I_{\mathrm{INP}}(k+n) = 1 \quad \text{for} \quad n = 0$$
$$I_{\mathrm{INP}}(k+n) = 0 \quad \text{for} \quad 0 < |n| \leq N. \quad (5)$$

For derivative filters, it is more adequate to calculate the response of a discrete Heaviside step function H_{S} (also called unit step function), which takes a value of 0 for all strictly negative values of k, and a value of 1 elsewhere:

$$H_{\mathrm{S}}(k) = 0 \quad k < 0$$
$$H_{\mathrm{S}}(k) = 1 \quad k \geq 0. \quad (6)$$

Again using an interval of $2N+1$ points centered at $z(k)$, the input step for which the response is needed will have a value of 0 for all samples below the central point $z(k)$, and a value of 1 for the central point and all samples above it:

$$I_{\mathrm{INP}}(k+n) = 0 \quad -N \leq n < 0$$
$$I_{\mathrm{INP}}(k+n) = 1 \quad 0 \leq n \leq N. \quad (7)$$

Though we considered an impulse (delta function) for smoothing filters and a step function (Heaviside step) for the derivative filters, for brevity we will hereafter call both types of response an "impulse response". For each altitude location considered, the impulse response consists of a vector whose length is at least as large as twice the number of filter coefficients used to smooth the signal at this location. The magnitude of the impulse response typically maximizes at the central point $z(k)$ of the filtering interval, and then decreases apart from this central value to a value of 0 for points outside the smoothing interval. Unlike the number of coefficients used by the filter, the width of the response (measured in number of bins) provides a quantitative measure of the actual smoothing impact of the filter on the signal at this location. The impulse response of a boxcar average is shown in Fig. 2 for several filter widths. Additional examples of impulse response for several smoothing and derivative filters are provided throughout this article and in the Supplement. Later in this paper, we will link vertical resolution, as it is often reported in lidar data files, to the impulse response width, and more precisely, to its full width at half maximum (FWHM).

2.2 The frequency approach: transfer function and gain

As in many signal processing applications, the frequency approach applied to lidar signal filtering or lidar-retrieved pro-

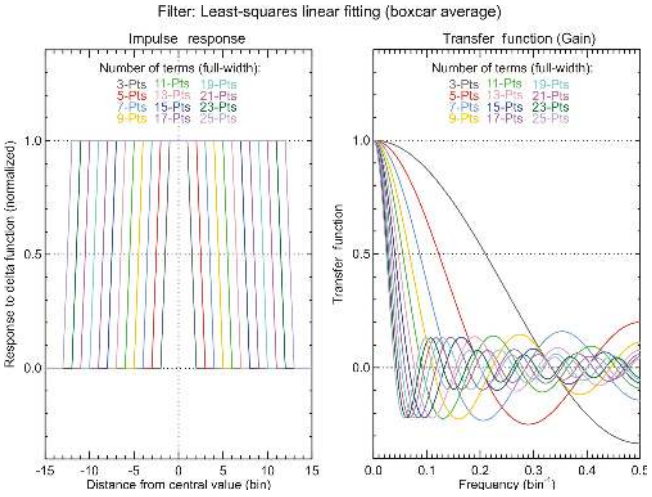

Figure 2. Impulse response (left) and gain (right) for a digital filter equivalent to fitting an unsmoothed signal with a polynomial of degree 1 or 2 using the least-squares method over an interval comprising $2N+1$ points (full width). Full widths represented in this figure range from 3 to 25 points. This least-squares filtering procedure is equivalent to a running average over $2N+1$ points (full width).

file filtering is a convenient mathematical framework. It is a more abstract, but very powerful tool allowing us to understand many hidden features of the smoothing and differentiation processes. A succinct, yet clear discussion of the required mathematical background is provided by Hamming (1989). Here, we will provide a brief review of this background relevant to our applications.

1. Aliasing: Any signal consisting of a finite number of equally spaced samples in the physical domain is an aliased representation of a sine and cosine function of frequency ω. Using the usual trigonometry formulae and the Euler identity, we can therefore express a single-frequency signal with unity amplitude in a complex form:

$$S(k) = e^{i\omega k}. \tag{8}$$

In the case of lidar, the signal (or the ozone or temperature profile) is a function of altitude range. The discretized independent variable is the vertical sampling bin k. The angular frequency ω (unit: radian bin^{-1}) is then connected to the frequency f (unit: bin^{-1}) and vertical wavelength L (unit: bin) by the relations as follows:

$$\omega = 2\pi f = \frac{2\pi}{L}. \tag{9}$$

2. Eigenfunctions and eigenvalues of a linear system: Any vector $\boldsymbol{x}$ of length M can be formed by linear combination of M linearly independent (orthogonal) eigenvectors $\boldsymbol{x}_i$:

$$\boldsymbol{x} = \sum_{i=1}^{M} a_i \boldsymbol{x}_i. \tag{10}$$

Furthermore, any nonzero and non-unity matrix $\mathbf{A}$ of dimension M by M multiplied by this vector can be expressed as the sum of the products of its elements by the corresponding eigenvalues λ_i:

$$\mathbf{A}\boldsymbol{x} = \sum_{i=1}^{M} a_i \mathbf{A}\boldsymbol{x}_i = \sum_{i=1}^{M} a_i \lambda_i \boldsymbol{x}_i. \tag{11}$$

3. Invariance under translation: The property of invariance under translation for the sine and cosine functions implies a direct relation between the signal expressed in its complex form and the eigenvalue $\lambda(\omega)$ for a given translation:

$$S(k+n) = e^{i\omega(k+n)} = e^{i\omega n} e^{i\omega k} = \lambda(\omega) S(k). \tag{12}$$

Using the above mathematical background, the filtered signal S_f presented in its classical form as a linear combination of the input signal S (Eq. 1) can be re-written in its frequency-approach form:

$$S_\mathrm{f}(k) = e^{i\omega k} \sum_{n=-N}^{N} c_n e^{i\omega n} = \lambda(\omega) e^{i\omega k} = \lambda(\omega) S(k). \tag{13}$$

The eigenvalue $\lambda(\omega)$ is independent of k and is called the transfer function, which can be computed in the frequency domain over a full cycle $[-\pi, \pi]$, or over half a cycle $[0, \pi]$ without losing information (symmetry of translation):

$$\lambda(\omega) = \sum_{n=-N}^{N} c_n e^{i\omega n} \quad 0 \le \omega \le \pi \text{ radian.bin}^{-1}. \tag{14}$$

We can express the transfer function more conveniently as a function of the frequency f:

$$H(f) = \sum_{n=-N}^{N} c_n e^{2i\pi f n} \quad 0 \le f \le 0.5\,\text{bin}^{-1}. \tag{15}$$

The maximum value $f = 0.5\,\text{bin}^{-1}$ is the Nyquist frequency, which corresponds to $L = 2$ bins, and which expresses the fact that the lidar instrument is unable to

exactly reproduce any feature of vertical wavelength smaller than twice the sampling resolution ($2\delta z$). The transformation described in Eq. (15) can easily be recognized as a well-known discrete Laplace transform, applied to the filter coefficients.

For a typical smoothing filter, the coefficients have even symmetry, i.e., $c_n = c_{-n}$ for all values of n. The complex transfer function can then be reduced to its real part. The gain of the filter G, which is the ratio of the actual transfer function $H(f)$ to the ideal transfer function $I(f)$ can then be written as follows:

$$G(f) = \frac{H(f)}{I(f)} = \frac{H(f)}{1} = c_0 + 2\sum_{n=1}^{N} c_n \cos(2\pi n f) \quad 0 \le f \le 0.5\,\mathrm{bin}^{-1}. \quad (16)$$

For a derivative filter, the $2N+1$ coefficients have odd symmetry, i.e., $c_n = -c_{-n}$ for all values of n and $c_0 = 0$. The complex transfer function is then reduced to its imaginary component:

$$H(f) = 2i\sum_{n=1}^{N} c_n \sin(2\pi n f). \quad (17)$$

With the complex notation of Eq. (8), the ideal vertical derivative of the signal can be written as follows:

$$S_\mathrm{f}(k) = i\omega e^{i\omega k} = 2i\pi f e^{i\omega k}. \quad (18)$$

The gain of the filter, then takes the following form:

$$G(f) = \frac{H(f)}{2i\pi f} = \frac{1}{\pi f}\sum_{n=1}^{N} c_n \sin(2\pi n f) \quad 0 \le f \le 0.5\,\mathrm{bin}^{-1}. \quad (19)$$

Referring back to Eq. (1), the gain provides a quantitative measure of the actual smoothing impact of the filter on the signal at a particular location $z(k)$ and for a given spectral component f.

Examples of gain for several smoothing and derivative filters are shown in Fig. 2 (right), and throughout the rest of this article as well as in the Supplement. Just like for the impulse response, later in this paper we will link vertical resolution as it is often reported in lidar data files to the cut-off frequency of digital filters, which is computed from the gain (see Sects. 3 and 4).

2.3 Example 1: least-squares fitting and boxcar average

Least-squares fitting is a well-established numerical technique used for many applications such as signal smoothing, differentiation, and interpolation. The relation between the number and values of the filter coefficients and the type of polynomial used to fit the signal can be found in many textbooks and publications (e.g., Birge and Weinberg, 1947; Savitsky and Golay, 1964; Steinier et al., 1972). In this paragraph we show that least-squares fitting with a straight line and boxcar averaging are the same filter. We start with the simple case of fitting five points with a straight line. We therefore look for the minimization of the following function:

$$F(a_0, a_1) = \sum_{n=-2}^{2} [S(k+n) - (a_0 + a_1 n)]^2. \quad (20)$$

This minimization is done by differentiating F with respect to each coefficient a_0 and a_1 and finding the root of each corresponding equation:

$$\begin{cases} 5a_0 + 0a_1 = \sum_{n=-2}^{2} S(k+n) \\ 0a_0 + 10a_1 = \sum_{n=-2}^{2} nS(k+n). \end{cases} \quad (21)$$

The value of the signal after filtering S_f is the mid-point value of the fitting function $a_0 + a_1 n$, which corresponds to the value of a_0 ($n = 0$):

$$S_\mathrm{f}(k) = a_0 = \frac{1}{5}\sum_{n=-2}^{2} S(k+n). \quad (22)$$

Identifying this equation to the generic Eq. (1), we deduce the five coefficients of the filter:

$$c_n = \frac{1}{5} \quad -2 \le n \le 2. \quad (23)$$

We recognize this result as the coefficients of a five-point boxcar average (five-point running average). The impulse response of this filter takes a value of 1 for all $|n|$ comprised between 0 and N, and a value of 0 elsewhere (see Fig. 2 left plot). Not surprisingly, all impulse response curves maximize at the central point ($n = 0$), and their full width at half maximum (FWHM) increases with the number of filter coefficients used.

Now switching to the frequency domain and using Eq. (14), the transfer function $\lambda(\omega)$ can be written in complex form:

$$\lambda(\omega) = \frac{1}{5}\left[e^{-2i\omega} + e^{-i\omega} + 1 + e^{i\omega} + e^{2i\omega}\right]. \quad (24)$$

The gain of the filter can be expressed as a function of frequency f:

$$G(f) = H(f) = \frac{1}{5} + 2\sum_{n=1}^{2} \frac{1}{5}\cos(2\pi n f), \quad (25)$$

which simplifies to

$$G(f) = H(f) = \frac{1}{5}\left[\frac{\sin(5\pi f)}{\sin(\pi f)}\right]. \quad (26)$$

We can generalize the above equation by fitting $2N+1$ points with a straight line, and we find

$$c_n = \frac{1}{2N+1} \quad -N \le n \le N \quad (27)$$

$$\lambda(\omega) = \frac{1}{2N+1} \quad (28)$$
$$\left[e^{-Ni\omega} + e^{-(N-1)i\omega} + \ldots + e^{-i\omega} + 1 + e^{i\omega} + \ldots + e^{(N-1)i\omega} + e^{Ni\omega}\right].$$

Alternatively, as a function of frequency, we find

$$G(f) = H(f) = \frac{1}{2N+1} + 2\sum_{n=1}^{N} \frac{\cos(2\pi n f)}{2N+1}, \quad (29)$$

which simplifies to

$$G(f) = H(f) = \frac{1}{2N+1}\left[\frac{\sin((2N+1)\pi f)}{\sin(\pi f)}\right]. \quad (30)$$

The gain functions for 3-point through 25-point boxcar average filters are plotted on the right-hand side of Fig. 2. The gain provides a more complete description of the smoothing ability of the filters because it provides a measure of noise attenuation as a function of frequency. All curves show a gain close to 1 for frequency values near 0 (low-pass filters), but they also show large ripples at larger frequencies when we approach the Nyquist frequency. The frequency f_0 of the first zero crossing (zero gain) is determined by the number of points used:

$$f_0 = \frac{1}{2N+1}. \quad (31)$$

The ripples observed on the right-hand side plot of Fig. 2 (the Gibbs phenomenon) are undesirable if the filter's objective is to remove the highest frequencies from the signal, which is the case for the lidar signal impacted by detection noise. The Gibbs ripples are predicted by Fourier theory because these digital filters have a finite number of coefficients, the equivalent in the physical domain of truncated Fourier series in the frequency domain. The strength of the frequency approach is to use Fourier theory, often refined by the concept of windowing, to minimize the Gibbs ripples. Detailing the underlying theory behind this behavior is beyond the scope of the present paper. Instead, below and in the Supplement, we simply provide the most common examples of modifications made to the filter coefficients, allowing an optimized design of a noise-reduction filter. More details on filters' windows can be found in, for example, Rabiner and Gold (1975).

2.4 Example 2: low-pass filter and cut-off frequency

If we were to consider an ideal low-pass filter with an infinite number of terms, the theoretical transfer function would have values between 0 and 1, representing the perfect gain of the filter (no ripples). The so-called transition region corresponds to the region where we want the transfer function to drop from a value of 1 at lower frequencies to a value of 0 at higher frequencies. The width of the transition region is the bandwidth. We can define the cut-off frequency of a low-pass filter as the frequency at which the transfer function equals 0.5. For most low-pass filters this is at the center of the transition region. To design a low-pass filter with the desired cut-off frequency f_C, we start with the initial conditions defining an ideal low-pass filter:

$$\begin{aligned} &G(f) = 1 \quad \text{for} \quad 0 < |f| < f_C \\ &G(f) = 0 \quad \text{for} \quad f_C < |f| < 0.5 \\ &G(f) = G(-f). \end{aligned} \quad (32)$$

Without getting into mathematical details, we find that these conditions are always true for a family of untruncated Fourier series with the following transfer function (Hamming, 1989):

$$H(f) = 2f_C + 2\sum_{n=1}^{\infty} \frac{\sin(2\pi n f_C)}{\pi n}\cos(2\pi n f). \quad (33)$$

Since we have to work with a finite number of samples, we truncate the series to a finite number of terms at the expense of producing Gibbs ripples. The real-world low-pass filter thus created has the following $2N+1$ coefficients and transfer function:

$$c_n = 2f_C \frac{\sin(2\pi n f_C)}{2\pi n f_C} \quad -N \le n \le N \quad (34)$$

$$G(f) = H(f) = 2f_C + 2\sum_{n=1}^{N} \frac{\sin(2\pi n f_C)}{\pi n}\cos(2\pi n f). \quad (35)$$

An example for $f_C = 0.15$ is shown for reference in Fig. 3. The impulse response (left) and gain (right) are shown for a filter full width comprised between 3 and 25 points. The first few Gibbs ripples always have the largest amplitude. Using a higher number of terms causes the ripples to be more concentrated near the transition region, and causes higher order ripples with a smaller amplitude to occur near the Nyquist frequency.

The gain curves show that the transition region is narrower than that observed for the boxcar average filters, but the Gibbs ripples appear on both sides of the transition region. Just like for the modified least-squares fitting, we can reduce the magnitude of the Gibbs ripples by modifying the filter coefficients, specifically by applying additional weights to the filter coefficients, a process called "windowing". Several examples of smoothing filters using Lanczos, von Hann, Hamming, Blackman, and Kaiser windows are provided for reference in the Supplement.

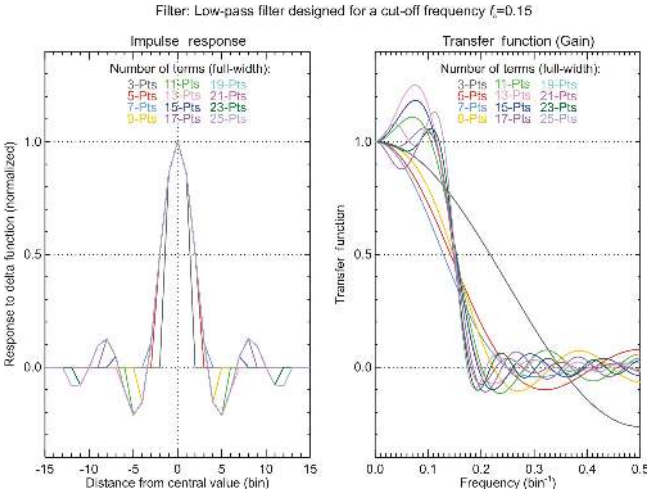

Figure 3. Impulse response and gain of low-pass filters using $2N+1$ coefficients (full width), and designed to have a cut-off frequency $f_C = 0.15$. Full widths range from 3 to 25 points.

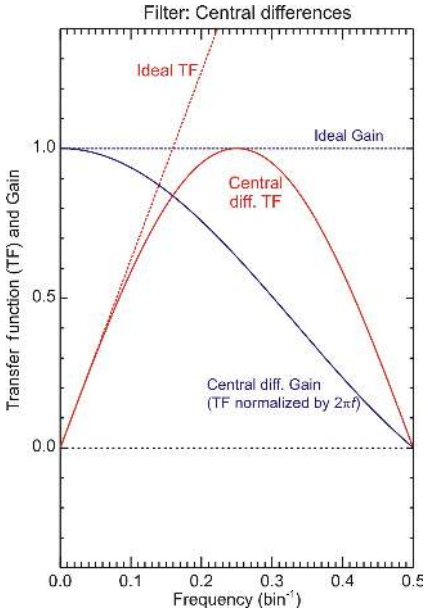

Figure 4. Transfer function (TF) and gain of the central difference digital filter. The gain (blue curve) is the transfer function (red curve) normalized by $2\pi f$, which is the real part of the ideal differentiator $i\omega$.

2.5 Example 3: central difference derivative filter

The simplest approximation of the derivative of a signal S at altitude $z(k)$ without a phase shift is the so-called three-point central difference, which can be written as follows:

$$S_f(k) = \frac{1}{2}\left(S(k+1) - S(k-1)\right). \tag{36}$$

Here we work in units of sampling bins rather than physical units; i.e., we assume the sampling resolution is $\delta z = 1$. We recognize the set of coefficients:

$$c_n = \frac{n}{2} \quad -1 \le n \le 1. \tag{37}$$

The transfer function, obtained from Eq. (36) is

$$\lambda(\omega) = \frac{1}{2}\left[-e^{-i\omega} + 0 + e^{i\omega}\right] = i\sin\omega. \tag{38}$$

Following the notation of Eq. (19) (odd symmetry), and using the values of the coefficients c_n (Eq. 37), we then compute the gain, i.e., the ratio of the value approximated by the central difference (Eq. 38) to the value of the ideal derivative (Eq. 18):

$$G(f) = \frac{H(f)}{2\pi f} = \frac{\sum_{n=1}^{1} \frac{n}{2}\sin(2\pi n f)}{\pi f} = \frac{\sin 2\pi f}{2\pi f}. \tag{39}$$

This equation shows that the central difference conserves the slope of the original signal for $f = 0$ only, and underestimates this slope for all other frequencies. Figure 4 shows the transfer function H (red solid curve) and gain G (blue solid curve) for the three-point central differences. Just like for the smoothing filters, we can design derivative low-pass filters that will conserve the slope of the signal for low values of frequency and attenuate the slope (or noise) for higher frequency values. Several examples are given in the Supplement.

3 Review of vertical resolution definitions used by NDACC lidar investigators

The filtering schemes or methods of several NDACC lidar investigators have been reviewed and compared in previous works, e.g., Beyerle and McDermid (1999) and Godin et al. (1999). These studies concluded that vertical resolution was not consistently reported between the various investigators. Here we briefly review the filtering schemes or methods used by various NDACC lidar investigators, and how vertical resolution is reported in their data files, as of 2011. This review provided critical input to the ISSI team to determine which definitions of vertical resolution are appropriate for use in a standardized way across the entire network (see Sect. 4).

- Observatoire de Haute-Provence (OHP, France), stratospheric ozone differential absorption lidar: A second-degree polynomial derivative filter (Savitsky–Golay derivative filter) is used (Godin-Beekmann et al., 2003). Vertical resolution is reported following a definition based on the cut-off frequency of the digital filter.
- Table Mountain (California) and Mauna Loa (Hawaii) stratospheric ozone and temperature lidars operated by

the Jet Propulsion Laboratory: Filtering is done by applying a fourth-degree polynomial least-squares fit (Savitsky–Golay derivative filter) to the logarithm of the signals for ozone retrieval. For the temperature profiles, a Kaiser filter is applied to the logarithm of the relative density profile. In both ozone and temperature cases, the cutoff frequency of the filter, reversed to the physical domain, is reported as vertical resolution (Leblanc et al., 2012).

- NASA GSFC mobile ozone DIAL STROZ instrument (United States): For ozone, a least-squares fourth-degree polynomial fit derivative filter (Savitsky–Golay derivative filter) is used. The definition of vertical resolution in the NDACC-archived data files is based on the impulse response of a delta function, by measuring the FWHM of the filter's response. For the temperature retrieval (Gross et al., 1997), the profiles are smoothed using a low-pass filter (Kaiser and Reed, 1977), and a simple ad hoc step function is used to define the values of the vertical resolution.

- Lauder (New Zealand) ozone lidar operated by RIVM (Netherlands): The definition of vertical resolution is based on the width of the fitting window used for the ozone derivation (Swart et al., 1994).

- OHP and Réunion Island (France) tropospheric ozone DIAL: A second-degree polynomial least-squares fit (Savitsky–Golay derivative filter) is used to filter the ozone measurements. The vertical resolution is reported as the cut-off frequency of the corresponding digital filter.

- Réunion Island (France) temperature lidar: A Hamming filter is applied to the temperature profile. The width of the window used is reported as the vertical resolution.

- University of Western Ontario (Canada) Purple Crow Lidar: For climatology studies, the temperature algorithm applies a combination of three-point and five-point boxcar average filters or a Kaiser filter on the temperature profiles (e.g., Argall and Sica, 2007). Similar filters are used in space or time for spectral analysis of atmospheric waves (e.g., Sica and Russell, 1999). Filter parameters are reported in the data files that are locally produced and distributed to the scientific user community. Previously, files were distributed to users with the type of filter and full bandwidth of the filter. The variance reduction of the filter is folded into the random uncertainties provided. The product of the data spacing and the filter bandwidth gives the full influence of the filter at each point. With the development of a temperature retrieval algorithm based on an optimal estimation method, vertical resolution of the temperature profile is now available as a function of altitude (Sica and Haefele, 2015).

- Tsukuba (Japan) ozone DIAL and temperature lidar: The algorithm uses second- and fourth-degree polynomial least-squares fits (Savitsky–Golay derivative filter). The vertical resolution is calculated from a simulation model that determines the FWHM of the impulse response to an ozone delta function. The FWHM is then mapped as a function of altitude. For temperature, a von Hann (or Hanning) window is used on the logarithm of the signal (B. Tatarov, personal communication, 2010).

- Garmisch-Partenkirchen (Germany) tropospheric ozone DIAL operated by IFU: The algorithm initially used linear and third-degree polynomial fits (Kempfer et al., 1994), and then since 1996 a combination of a linear fit and a Blackman-type window (Eisele and Trickl, 2005; Trickl, 2010). The latter filter has a reasonably high cut-off frequency and does not transmit as much noise as the derivative filters used earlier at IFU (Kempfer et al., 1994). To report vertical resolution in the data files, a Germany-based standard definition of vertical resolution is used, following the Verein Deutscher Ingenieure DIAL guideline (VDI, 1999). This definition is based on the impulse response to a Heaviside step function. The vertical resolution is given as the distance separating the positions of the 25 and 75 % in the rise of the response, which is approximately equivalent to the FWHM of the response to a delta function. In the case of the ozone DIAL, the vertical resolution of both the Blackman-type filter used and the combined least-squares derivative plus Blackman filter. A vertical resolution of 19.2 % of the filtering interval was determined. For small intervals the latter value may change; i.e., the least-squares fit for determining the derivative is executed over just a few data points. For comparison, an arithmetic average yields a vertical resolution of 50 % of the filtering interval.

Having reviewed the vertical resolution definitions and schemes used across NDACC and elsewhere, three definitions or approaches can be clearly identified. The first definition is the number of filter coefficients used, the second definition is based on the cut-off frequency of the filter used, and the third definition is based on the width of the impulse response of the filter used. Those definitions were already mentioned by Beyerle and McDermid (1999), but no decision was made within NDACC to find a standardized approach across the network. The present article and its Supplement show that not all filters have the same properties, and that the characteristics of a filter do not simply depend on the number of coefficients used, but instead on a combination of the number of coefficients and their values. Indeed, Fig. 5 below shows the gain of several filters having the same number of coefficients (five points for the smoothing filters on the left-hand plot, and seven points for the derivative filters on the right-hand plot). It is obvious that, depending on the filter and/or window used, the transition region between

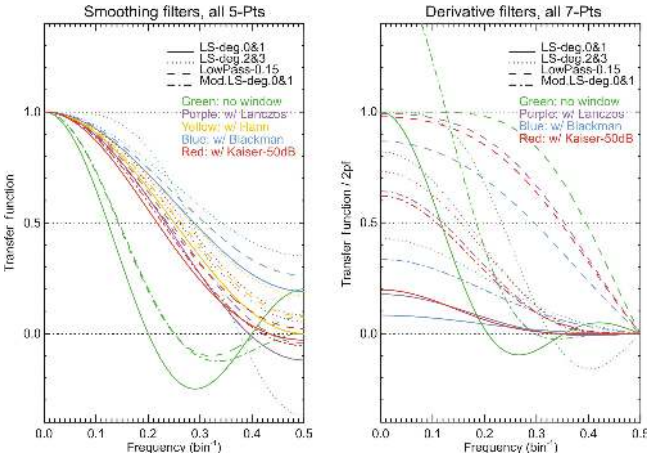

Figure 5. Transfer function (gain) of several smoothing (left) and derivative (right) filters, all with exactly the same number of coefficients, $2N+1$ (five-point full width for the smoothing filters and seven-point full width for the derivative filters).

passband and stopband is located at very different frequencies. In the examples shown, it is located between $f = 0.12$ and $f = 0.35$ for smoothing filters, while the derivative filters show considerably more variability.

Finding transition regions at different frequencies means that the smoothing effect of the filters on the signal is different, even though the number of coefficients is the same. A vertical resolution definition based on the number of coefficients is therefore not reliable. Instead we need to choose a standardized definition based on objective parameters that are directly related to the effect a filter has on the signal. Two such definitions are proposed thereafter, definitions that are similar or closely related to the two remaining definitions identified in the present section.

4 Proposed standardized vertical resolution definitions for the NDACC lidars

The two definitions proposed here were chosen because they provide a straightforward characterization of the underlying smoothing effect of filters (see Sect. 2), and they appear to have already been used by a large number of NDACC investigators (see Sect. 3). The first definition is based on the width of the impulse response of the filter. The second definition is based on the cut-off frequency of the filter. Further justification for the choice of either definition is provided at the end of the present section.

4.1 Definition based on the FWHM of a finite impulse response

The full width at half maximum (FWHM) of an impulse response, as introduced in Sect. 2, is computed by measuring the distance (in bins) between the two points at which the response magnitude falls below half of its maximum amplitude. The NDACC lidar standardized definition of vertical resolution proposed here is computed from the response I_{OUT} of a Kronecker delta function for smoothing filters and a Heaviside step function for derivative filters. Because of the dynamic range of the lidar signals (or ozone or temperature profiles), we assume that the number of filter coefficients could vary with altitude. Therefore, the standardized vertical resolution is estimated separately for each altitude $z(k)$ in the following manner.

1. Define and/or identify the $2N(k)+1$ filter coefficients $c(k,n)$ used to perform the smoothing or differentiation operation on the signal (lidar counts, ozone or temperature profile):

$$S_{\mathrm{f}}(k) = \sum_{n=-N(k)}^{N(k)} c(k,n) S(k+n) \quad \text{for} \quad N(k) < k < nk - N(k). \tag{40}$$

2. Construct an impulse function of finite length $2M(k)+1$ to be convolved with the filter coefficients. The value of $M(k)$ is not critical but has to be greater than or equal to $N(k)$. For smoothing filters, the impulse function is the Kronecker delta function which can be written as follows:

$$I_{\mathrm{INP}}(k,m) = \delta_0(m) \ \text{ with } \ -M(k) \le m \le M(k) \quad \text{and} \quad N(k) \le M(k) \le \frac{nk-1}{2}. \tag{41}$$

This function equals 1 at the central point ($m = 0$) and equals 0 everywhere else. For derivative filters, the impulse function is the Heaviside step function which can be written as follows:

$$I_{\mathrm{INP}}(k,m) = H_{\mathrm{S}}(m) \ \text{ with } \ -M(k) \le m \le M(k) \quad \text{and} \quad N(k) \le M(k) \le \frac{nk-1}{2}. \tag{42}$$

This function equals 0 at all locations below the central point ($m < 0$) and equals 1 everywhere else.

3. Convolve the filter coefficients with the impulse function in order to obtain the impulse response I_{OUT}:

$$I_{\mathrm{OUT}}(k,m) = \sum_{n=-N(k)}^{N(k)} c(k,n) I_{\mathrm{INP}}(k,m+n). \tag{43}$$

4. Estimate the full width at half maximum (FWHM) of the impulse response I_{OUT} by measuring the distance Δm_{IR}, in bins, between the two points (located on each

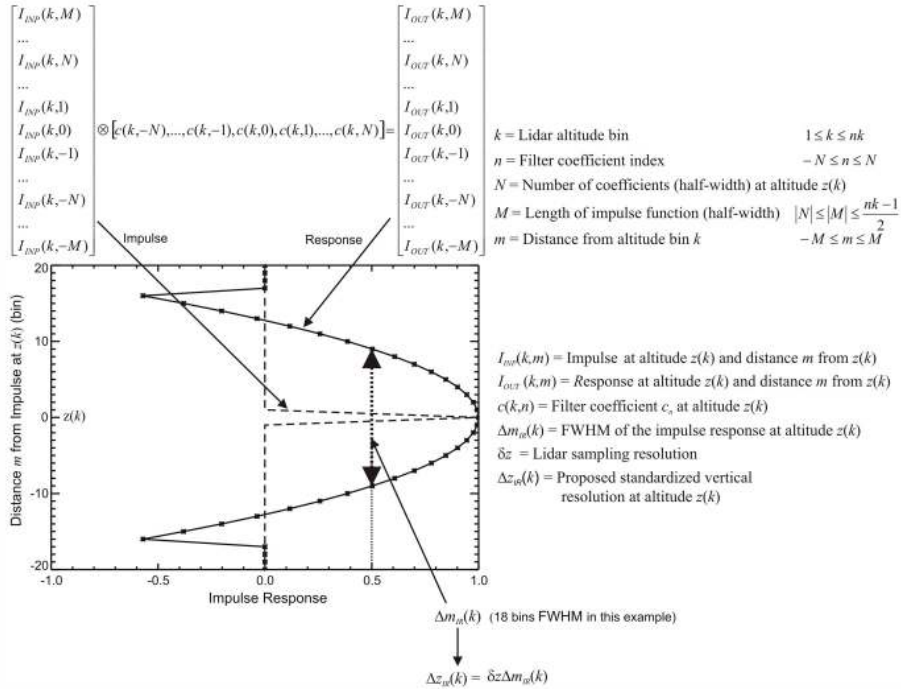

Figure 6. Schematics summarizing the procedure that should be followed to compute the standardized vertical resolution with a definition based on the impulse response FWHM Δz_{IR}.

side of the central bin) where the response magnitude falls below half of the maximum amplitude:

$$I_{\mathrm{OUT}}(k, m_1(k)) = 0.5\max\left(I_{\mathrm{OUT}}(k, m_i)\right) \quad \text{for all} \quad -M(k) \le m_i \le 0$$
$$I_{\mathrm{OUT}}(k, m_2(k)) = 0.5\max\left(I_{\mathrm{OUT}}(k, m_i)\right) \quad \text{for all} \quad 0 \le m_i \le M(K) \tag{44}$$
$$\Delta m_{\mathrm{IR}}(k) = |m_1(k) - m_2(k)|\,. \tag{45}$$

For a successful identification of the FWHM, the impulse response should have only two points where its value falls below half of its maximum amplitude, which is normally the case for all smoothing and derivative filters used within their prescribed domain of validity (see examples in Sect. 2 and in the Supplement). In the event that more than two points exist, the two points farthest from the central bin should be chosen in order to yield the most conservative estimate of vertical resolution.

5. Compute the standardized vertical definition Δz_{IR} as the product of the lidar sampling resolution δz and the estimated FWHM:

$$\Delta z_{\mathrm{IR}}(k) = \delta z \Delta m_{\mathrm{IR}}(k). \tag{46}$$

Figure 6 summarizes the estimation procedure. The unsmoothed signal yields a FWHM of one bin. This result is derived by considering null coefficients everywhere except at the central point ($m = 0$), where the coefficient equals 1. The intercept theorem within the triangles formed by the impulse response at the central point and its two adjacent points ($m = -1$ and $m = 1$) yields a FWHM of one bin, and the standardized vertical resolution using the present impulse-response-based definition will always be greater than or equal to the sampling resolution:

$$\Delta z_{\mathrm{IR}}(k) \ge \delta z \quad \text{for all} \quad k. \tag{47}$$

When several filters are applied successively to the signal, the response of the filter must be computed each time a filtering operation occurs, and vertical resolution needs to be computed only after the last filtering occurrence. The process can be summarized as follows: a first impulse response is computed with the first filtering operation. If no further filtering occurs, the impulse response is used to determine the FWHM and vertical resolution. If a second filtering operation occurs, the impulse response is used as input signal, and a second response is computed from the convolution of this input signal with the coefficients of the second filter. If no further filtering occurs, the second response is used to determine the FWHM and vertical resolution. If a third filtering operation occurs, the response output from the second convolution is used as input signal of the third convolution, and so on until no more filtering is applied to the signal. Vertical resolution is always

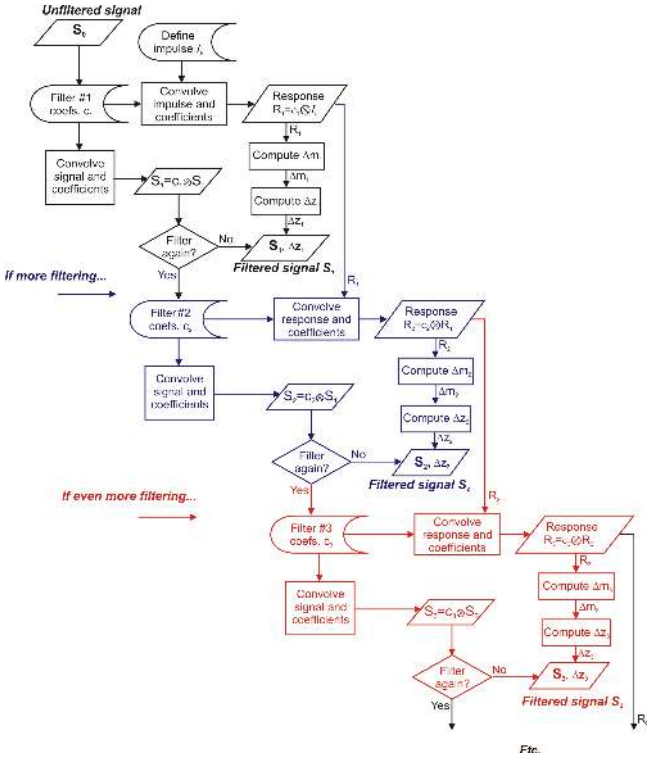

Figure 7. Schematics summarizing the procedure that should be followed to compute the standardized vertical resolution with a definition based on impulse response when the signal or profile is filtered multiple times.

computed from the final output response, i.e., after the final filtering operation. Figure 7 summarizes the procedure.

4.2 Definition based on the cut-off frequency of digital filters

The cut-off frequency of digital filters is defined as the frequency at which the value of the filter's gain is 0.5, typically located at the center of the transition region between the passband and the stopband (see Sect. 2). The NDACC lidar standardized definition proposed here is computed from the cut-off frequency f_C, which is determined from the gain of the filter obtained by applying a Laplace transform to the coefficients of the filter used. Once again, because of the dynamic range of the lidar signals, filtering a lidar signal (or ozone/temperature profile) often requires using a number of filter coefficients which vary with altitude. Starting with a lidar signal (or ozone or temperature profile) S composed of nk equally spaced elements in altitude, the standardized vertical resolution is estimated separately for each altitude $z(k)$. The procedure can be summarized as follows for each altitude considered.

1. Define and/or identify the $2N(k)+1$ filter coefficients $c(k,n)$ used to perform the smoothing or differentiation operation on the lidar signal (or on the ozone or temperature profile) at altitude:

$$S_f(k) = \sum_{n=-N(k)}^{N(k)} c(k,n)S(k+n) \quad \text{for} \quad N(k) < k < nk - N(k). \tag{48}$$

2. Apply the Laplace transform to the coefficients to determine the filter's transfer function and gain. For non-derivative smoothing filters, the coefficients have even symmetry, i.e., $c(k,n) = c(k,-n)$, and the gain is written as follows:

$$G(k,f) = H(k,f) = c(k,0) + 2\sum_{n=1}^{N(k)} c(k,n)\cos(2\pi nf) \quad 0 < f < 0.5. \tag{49}$$

For derivative filters, the coefficients have odd symmetry, i.e., $c(k,n) = -c(k,-n)$, and if δz is the sampling resolution, the gain can be written as follows:

$$G(k,f) = \frac{H(k,f)}{2\pi f} = 2\sum_{n=1}^{N(k)} c(k,n)\frac{\sin(2\pi nf)}{2\pi f} \quad 0 < f < 0.5. \tag{50}$$

For a successful cut-off frequency estimation process, the gain must be computed with normalized coefficients c_n; that is, the coefficients must meet the following normalization condition:

$$\sum_{n=-N(k)}^{N(k)} c(k,n) = 1 \quad \text{for smoothing filters}$$
$$2\sum_{n=1}^{N(k)} nc(k,n) = 1 \quad \text{for derivative filters.} \tag{51}$$

3. Estimate the cut-off frequency, i.e., the frequency f_C at which the gain equals 0.5:

$$G(k, f_C(k)) = 0.5 \quad 0 < f_C(k) \leq 0.5. \tag{52}$$

For a successful identification, the gain should have only one crossing with the 0.5 line, typical for the smoothing and derivative filters used within their prescribed domain of validity for lidar retrieval systems. In the event that several crossings exist, the frequency closest to zero should be chosen to ensure that the most conservative estimate of vertical resolution is retained.

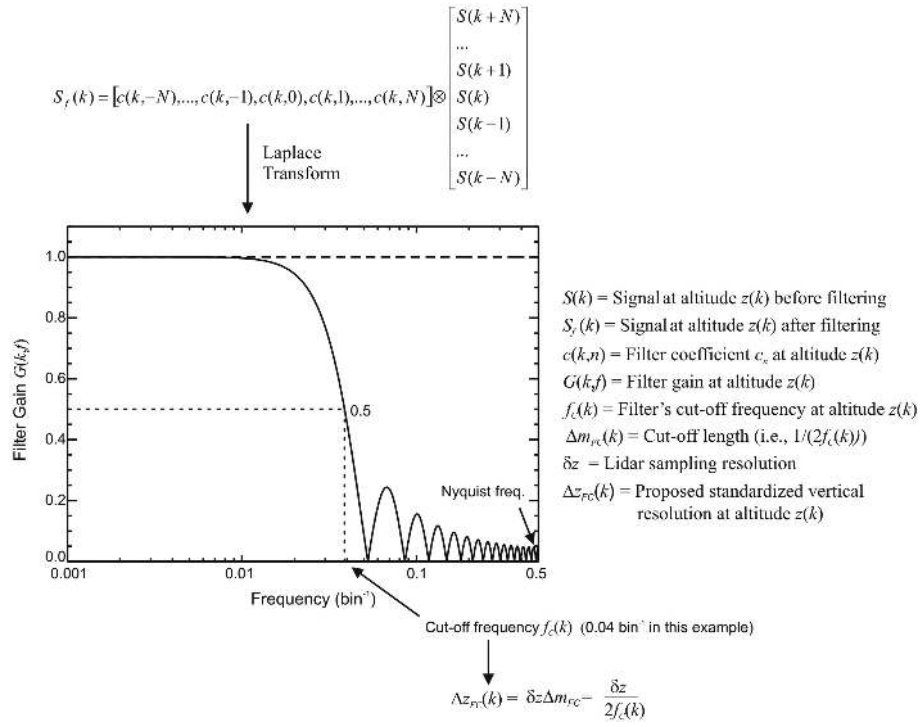

Figure 8. Schematics summarizing the procedure that should be followed to compute the standardized vertical resolution with a definition based on cut-off frequency Δz_{FC}.

4. Calculate the cut-off length Δm_{FC} (unit: bins), i.e., the inverse of the frequency f_{C} normalized to the sampling width:

$$\Delta m_{\mathrm{FC}}(k) = \frac{1}{2 f_{\mathrm{C}}(k)}. \tag{53}$$

5. Compute the standardized vertical definition Δz_{FC} as the product of the lidar sampling resolution δz and the cut-off length Δm_{FC} at that altitude:

$$\Delta z_{\mathrm{FC}}(k) = \delta z \Delta m_{\mathrm{FC}}(k) = \frac{\delta z}{2 f_{\mathrm{C}}(k)}. \tag{54}$$

Figure 8 summarizes this estimation procedure. The factor of 2 present in the denominator of Eq. (53) is usually not used in spectral analysis, when it is normally assumed that the minimum vertical scale that can be resolved by the instrument is twice the sampling resolution (Nyquist criterion). However, it is included here in order to harmonize the numerical values with the values computed using the impulse response definition. Using the present proposed definition, an unsmoothed signal yields a vertical resolution of δz and the standardized vertical resolution will always be at least equal to the sampling resolution:

$$\Delta z_{\mathrm{FC}}(k) \geq \delta z \quad \text{for all} \quad k. \tag{55}$$

When several filters are applied successively to the signal, the transfer function must be computed each time a filtering operation occurs, but vertical resolution needs to be computed only after the last filtering occurrence. The process can be summarized as follows: a first transfer function (or gain) is computed with the first filtering operation. When the second filtering operation occurs, the gain computed using the coefficients of the second operation is multiplied by the gain computed during the first filtering operation. If no further filtering occurs, the result of this product is the gain that should be used to determine the cut-off frequency and vertical resolution. If a third filtering operation occurs, the product of the first and second gain must be multiplied by the third gain, and so on until no more filtering occurs. When the final filtering operation is reached, vertical resolution can be computed from the final output gain. Figure 9 summarizes the procedure.

4.3 Comparison between the impulse-response-based (IR) and cut-off frequency-based (CF) definitions

In Sects. 4.1 and 4.2, we showed that, when using the proposed definitions based on impulse response and cut-off frequency, the standardized vertical resolution of an unsmoothed lidar signal (or profile) is equal to the lidar sampling resolution. However, this equality between the two definitions is not perfect for all filters. Here, we show that for most filters, there is a well-defined proportionality relation

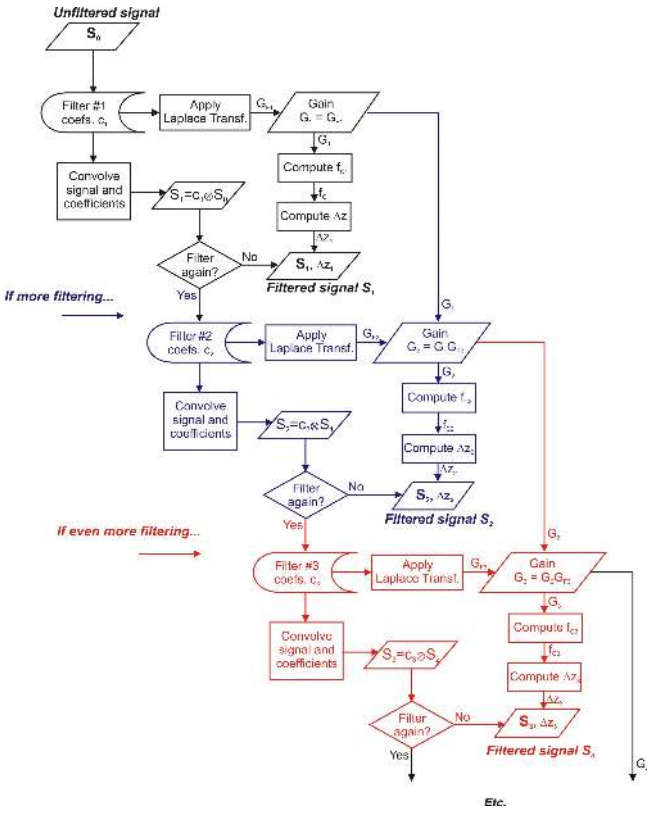

Figure 9. Schematics summarizing the procedure that should be followed to compute the standardized vertical resolution with a definition based on cut-off frequency when the signal or profile is filtered multiple times.

between the two definitions, but we also show that the proportionality factor depends on the type of filter used. In the rest of this section, for convenience, we will work with vertical resolutions normalized by the sampling resolution (unit: bins). The results are therefore shown as cut-off width Δm_{FC} and impulse response FWHM Δm_{IR} instead of Δz_{FC} and Δz_{IR} respectively, which is equivalent to assuming $\delta z = 1$.

Figure 10 shows, for the smoothing filters introduced in Sect. 2 and in the Supplement, the correspondence between the standardized vertical resolutions (in bins) computed using the cut-off frequency and the impulse response, for full widths comprised between 3 and 25 points. The black solid circle at coordinate (1,1) indicates the vertical resolution for the unsmoothed signal (or profile). The gray horizontal and vertical dash-dotted lines indicate the highest possible vertical resolutions for the impulse-response-based and cut-off frequency-based definitions respectively. The gray dotted straight lines indicate the result of the linear regression fits between the two definitions, and the numbers at their extremities are the values of the slope for three of the four types of filters used. There is no proportionality between the two definitions for the low-pass filters (diamonds) because the cut-off frequency is prescribed for this type of filter. Note

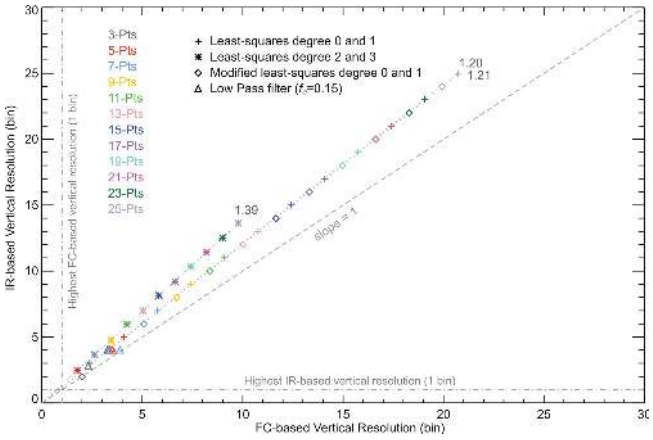

Figure 10. Comparison between the cut-off frequency-based and the impulse-response-based standardized vertical resolutions for several smoothing filters introduced in Sect. 2 and in the Supplement. The numbers at the end of the dotted straight lines indicate the proportionality constant (slope) between the two definitions for three of the four types of filters used. There is no such proportionality for the low-pass filter (prescribed cut-off frequency).

that the factors of 1.2 and 1.39 do not correspond to the ratio of 1.0 that is assumed for the unsmoothed signal. Very similar conclusions can be drawn for the derivative filters, as demonstrated by Fig. 11 (which is similar to Fig. 10 but for the derivative filters introduced in Sect. 2 and in the Supplement).

Figure 12 is similar to Fig. 10, but this time shows the period after the filters were convolved with the windows introduced in the Supplement. The windows change the proportionality constant between the two definitions, but this constant appears to be approximately the same for a given window, specifically around 1.04 for Lanczos, 1.0 for von Hann, 0.92 for Blackman, and 1.0 for Kaiser (50 dB). Table 1 summarizes the proportionality constants for all filters and all windows introduced in Sect. 2 and in the Supplement.

Figure 13 shows, for the filters introduced in Sect. 2 and in the Supplement, the correspondence between the two proposed standardized vertical resolutions (in bins) and the number of filter coefficients used (full widths comprised between 3 and 25 points). The dashed gray line represents unity slope (i.e., one bin for one filter coefficient), and the numbers at the end of the red and blue dotted straight lines indicate the slope of the linear fit applied to the paired points for each definition. As expected for a boxcar average, the impulse-response-based definition yields a vertical resolution (in bins) that is equal to the number of terms used (see Fig. 2). This is a particular case for which reporting vertical resolution using the number of filter terms yields a result identical to the impulse-response-based standardized definition. Note that for low-pass filters with a prescribed cut-off frequency, the vertical resolution does not depend at all on the number of filter terms used (right-hand plot).

Table 1. Proportionality factor between the impulse-response-based and the cut-off frequency-based definitions of vertical resolution for the filters and windows introduced in Sect. 2 and in the Supplement.

Ratio $\Delta z_{IR}/\Delta z_{FC}$	LS[a] and MLS[b] deg. 0–1	LS deg. 2–3	LS deriv. deg. 1–2	LS deriv. deg. 3–4	LS deriv. deg. 5–6
No window	1.20	1.39	1.12	1.23	1.24
$w/$ Lanczos window	1.03	1.04	0.98	0.97	1.07
$w/$ von Hann window	1.00	0.98	/	/	/
$w/$ Blackman window	0.92	0.94	0.92	0.92	0.95
$w/$ Kaiser 50 dB window	0.98	1.02	0.97	0.98	1.05

[a] LS: least-squares. [b] MLS: modified least-squares.

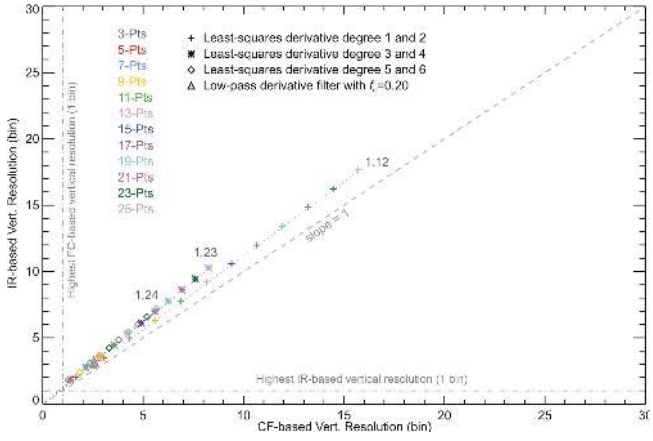

Figure 11. Same as Fig. 10, but for derivative filters (Sect. 2 and the Supplement).

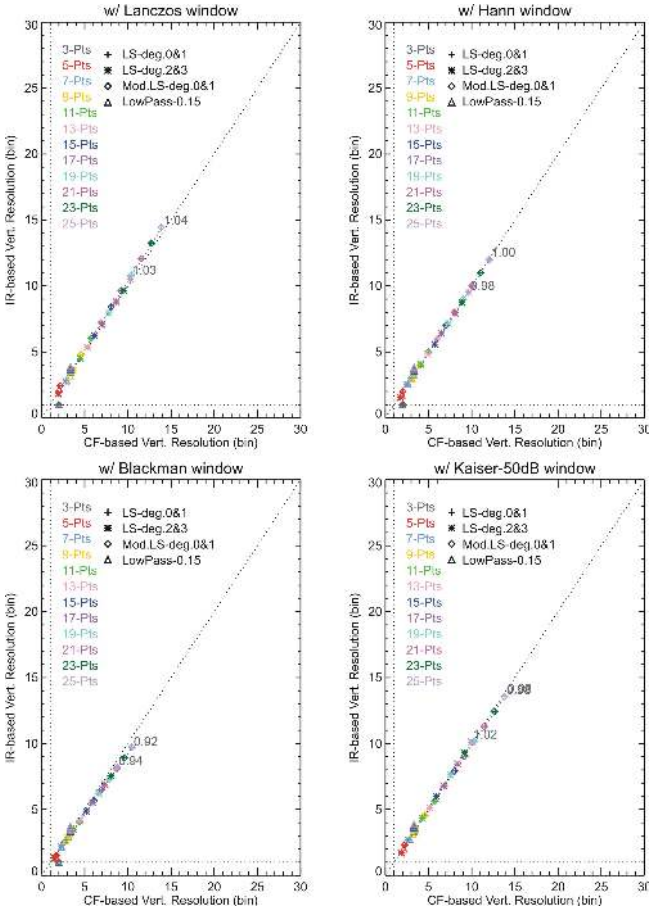

Figure 12. Same as Fig. 10, but for the filters being convolved with the four windows introduced in the Supplement.

Figure 14 is similar to Fig. 13, but this time shows the period after convolution by a von Hann window. Except for the low-pass filter, there is a factor of approximately 2 between the number of terms used by the filter and the vertical resolution for both definitions. Figure 15 is similar to Fig. 13, but for three selected derivative filters.

The factors between the vertical resolutions (in bins) and the number of filter coefficients are compiled in Tables 2 and 3 for the cut-off frequency-based and the impulse-response-based definitions, respectively.

In this section, it was shown that each recommended definition of vertical resolution yields its own numerical values; i.e., for the same set of filter coefficients, the reported standardized vertical resolution will likely have two different numerical values depending on the definition used. Unfortunately, there is no unique proportionality factor between the two definitions that could be used for all digital filters in order to obtain a unified homogenous definition yielding identical values. However, after reviewing this homogeneity problem, the ISSI team concluded that both definitions should still be recommended because the computed values remain close, specifically within 10 % if using windows and within 20 % if not using windows, and because each definition is indeed useful for specific applications. For example, the cut-off frequency-based definition is particularly useful for studies of gravity waves from lidar temperature measurements because it can provide, through the transfer function, spectral information that can help interpret quantitative findings on the amplitude and wavelength of lidar-observed waves. This type of information is not available when using the impulse-response-based definition. On the other hand, the impulse-

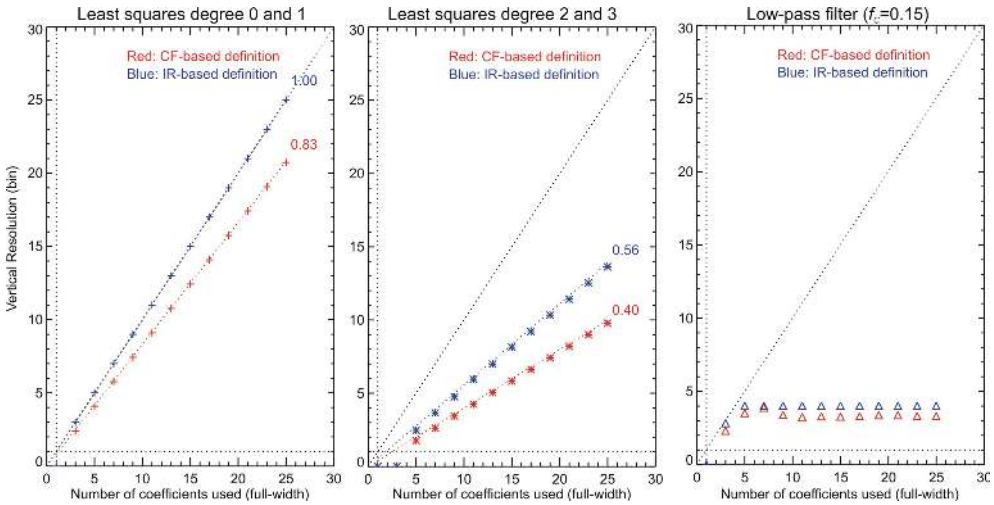

Figure 13. Correspondence between cut-off frequency-based (red) and impulse-response-based (blue) vertical resolution (in bins), and the number of filter coefficients used (full width), for three filters introduced in Sect. 2. The dashed gray line represents unity slope (i.e., one bin for one point), and the numbers at the end of the red and blue dotted straight lines indicate the slope of the linear fit applied to the paired points for each definition.

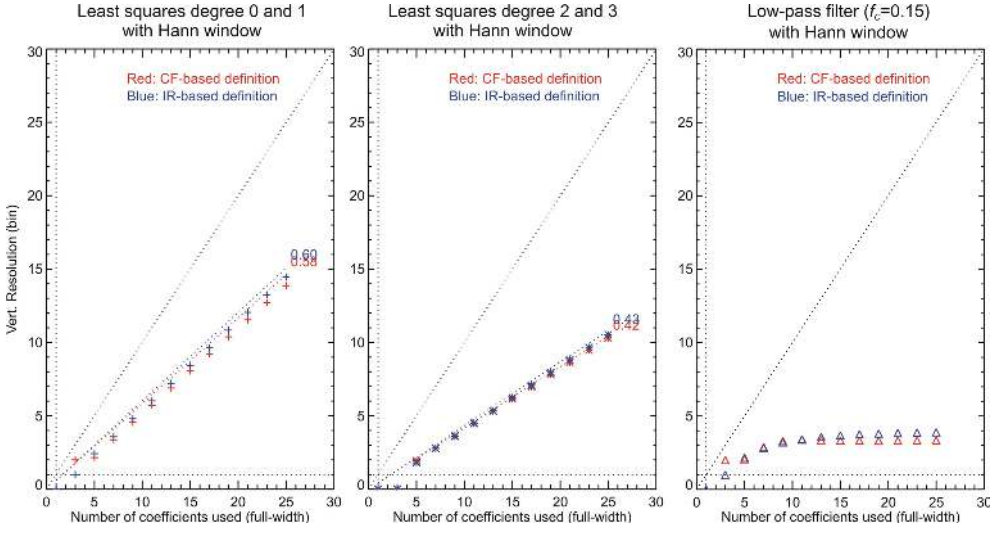

Figure 14. Same as Fig. 13, but this time for the period after convolution by a von Hann window.

response-based definition is widely used in atmospheric remote sensing, and it provides information in the physical domain similar to that provided through the averaging kernels of optimal estimation methods (e.g., microwave radiometer measurement of ozone or temperature).

4.4 Additional recommendations to ensure full traceability

When archiving the ozone or temperature profiles, reporting values of vertical resolution using a standardized definition such as Δz_{FC} or Δz_{IR} constitutes an important improvement from other non-standardized methods, such as the number of points used by the filter. However, using one standardized definition or even both standardized definitions proposed here still does not characterize the complete smoothing effect of the filter on the signal. For full traceability, it is necessary to provide, for each altitude point, either the set of filter coefficients used (for one-time smoothing cases) or to provide the complete transfer function or impulse response. This information can be critical when comparing the lidar profiles with profiles from other instruments, or when working with averaging kernels used for other measurements.

If the data provider chooses to report standardized vertical resolution information based on the impulse response definition, the complete vertical resolution information should include the following:

Table 2. Proportionality factor between the number of filter coefficients (full width) and vertical resolution based on cut-off frequency (in bins) for the filters and windows introduced in Sect. 2 and in the Supplement.

Ratio $\Delta m_{FC}/(2N+1)$	LS[a] and MLS[b] deg. 0–1	LS deg. 2–3	LS deriv. deg. 1–2	LS deriv. deg. 3–4	LS derive. deg. 5–6
No window	0.83	0.40	0.63	0.34	0.26
$w/$ Lanczos window	0.58	0.42	0.51	0.40	0.30
$w/$ von Hann window	0.50	0.43	/	/	/
$w/$ Blackman window	0.43	0.36	0.40	0.35	0.30
$w/$ Kaiser 50 dB window	0.57	0.41	0.50	0.39	0.30

[a] LS: least-squares. [b] MLS: modified least-squares.

Table 3. Proportionality factor between the number of filter coefficients (full width) and vertical resolution based on impulse response FWHM (in bins) for the filters and windows introduced in Sect. 2 and in the Supplement.

Ratio $\Delta m_{IR}/(2N+1)$	LS[a] and MLS[b] deg. 0–1	LS deg. 2–3	LS deriv. deg. 1–2	LS deriv. deg. 3–4	LS derive. deg. 5–6
No window	1.00	0.56	0.71	0.42	0.33
$w/$ Lanczos window	0.60	0.43	0.50	0.38	0.32
$w/$ von Hann window	0.50	0.39	/	/	/
$w/$ Blackman window	0.41	0.34	0.37	0.31	0.29
$w/$ Kaiser 50 dB window	0.56	0.42	0.49	0.37	0.31

[a] LS: least-squares. [b] MLS: modified least-squares.

1. a vector Δz_{IR} of length nk containing the standardized vertical resolution values at each altitude, as proposed in Sect. 4.2;

2. a two-dimensional array of size $nk \times nm$ containing the full impulse response used to estimate the FWHM ($nm = 2M + 1$ is the full length of the impulse function convolved with the filter coefficients, and a recommended value is $nm = nk$);

3. a vector m of length nm containing the distance (in bins) from the central bin at which the response is reported;

4. metadata information clearly describing the nature of the reported vectors and arrays.

If the data provider chooses to report standardized vertical resolution information based on the cut-off frequency definition, the complete vertical resolution information should therefore include the following:

1. a vector Δz_{FC} of length nk containing the standardized vertical resolution values at each altitude, as proposed in Sect. 4.1;

2. a two-dimensional array of size $nk \times nf$ containing the gain used to estimate the cut-off frequency (nf is the number of frequencies used when applying a Laplace transform to the filter coefficients, and a recommended value is $nf = nk$);

3. a vector $\boldsymbol{f}$ of length nf containing the values of frequency at which the gain is reported;

4. metadata information clearly describing the nature of the reported vertical resolution vector, frequency vector, and two-dimensional gain array.

If the data provider chooses to report standardized vertical resolution based on both the impulse response definition and the cut-off frequency definition, the complete vertical resolution information should include the following:

1. a vector $\boldsymbol{\Delta z}_{IR}$ of length nk containing the standardized vertical resolution values at each altitude, as proposed in Sect. 4.2;

2. a two-dimensional array of size $nk \times nm$ containing the full impulse response used to estimate the FWHM ($nm = 2M + 1$ is the full length of the impulse function convolved with the filter coefficients, and a recommended value is $nm = nk$);

3. a vector $\boldsymbol{m}$ of length nm containing the distance (in bins) from the central bin at which the response is reported;

4. a vector $\boldsymbol{\Delta z}_{FC}$ of length nk containing the standardized vertical resolution values at each altitude, as proposed in Sect. 4.1;

5. a two-dimensional array of size $nk \times nf$ containing the gain used to estimate the cut-off frequency (nf is the

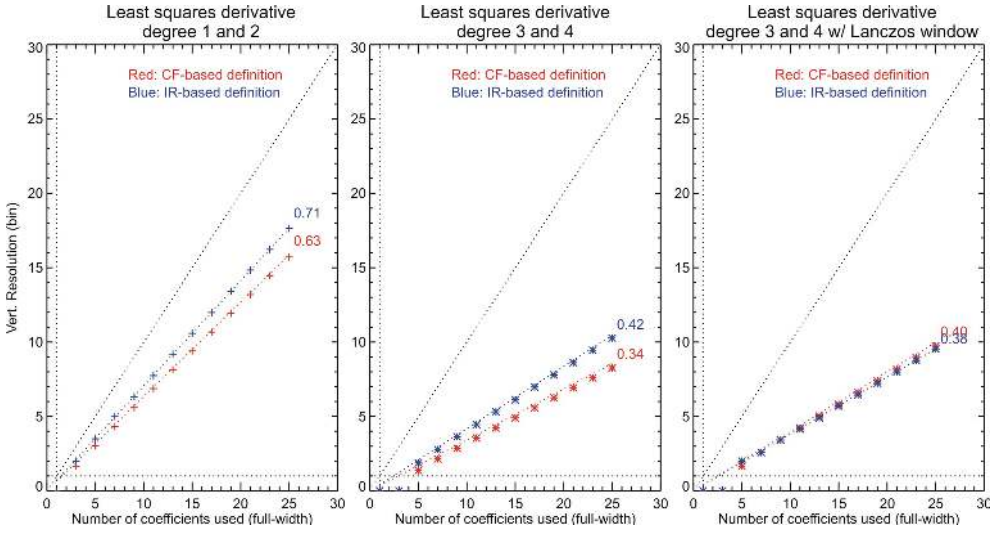

Figure 15. Same as Fig. 13 but for selected derivative filters and windows from Sect. 2 and the Supplement.

number of frequencies used when applying a Laplace transform to the filter coefficients, and a recommended value is $nf = nk$);

6. a vector $\boldsymbol{f}$ of length nf containing the values of frequency at which the gain is reported;

7. metadata information describing clearly the nature of all reported vectors and arrays.

4.5 Practical implementation within NDACC

Numerical tools were developed and provided to the NDACC principal investigators (PIs) in order to facilitate the implementation of the network-wide use of the proposed standardized definitions. These tools consist of easy-to-use plug-in routines written in IDL, MATLAB and FORTRAN, which convert a set of filter coefficients into the needed standardized values of vertical resolution following one or the other proposed definitions. The tools are written in such a way that they can be called in a lidar data processing algorithm each time a smoothing and/or differentiating operation occurs. The routines can handle multiple smoothing and/or differentiating operations applied successively throughout the lidar data processing chain, as described in Sects. 4.1 and 4.2. The routines are available on the NDACC lidar working group website (http://ndacc-lidar.org/), or upon request from the first author (thierry.leblanc@jpl.nasa.gov).

The routine "NDACC_ResolIR" computes vertical resolution values with a definition based on the FWHM of the filter's impulse response. When the routine is called for the first time in the data processing chain, the sampling resolution and the coefficients of the filter are the only input parameters of the routine. The routine convolves the coefficients with an impulse (delta function for smoothing filters and Heaviside function for derivative filters) to obtain the filter's impulse response, and then identifies the full width at half maximum (FWHM) of this response. The response and the value of vertical resolution are the output parameters of the routine. The product of the response full width by the sampling resolution is performed inside the routine. When a second call to the routine occurs (second smoothing occurrence), the vertical resolution output from the first call is no longer used. Instead, the response output from the first call is used as input parameter for the second call, together with the sampling resolution and the coefficients of the second filter. The input response is convoluted with the coefficients of the second filter to obtain a second response. The routine identifies the FWHM of this new response. Once again the vertical resolution is computed inside the routine by calculating the product of the new FWHM and the sampling resolution. The new response and the new vertical resolution are the output parameters of the routine after the second call. The procedure is repeated as many times as needed, i.e., as many times as a smoothing or differentiation operation occurs.

The routine NDACC_ResolDF computes vertical resolution values with a definition based on the cut-off frequency of a digital filter. When the routine is called for the first time in the data processing chain, the sampling resolution and the coefficients of the filter are the only input parameters of the routine. The routine applies a Laplace transform to the coefficients to obtain the filter's gain, and then identifies the cut-off frequency. The inverse of the doubled cut-off frequency is multiplied by the sampling resolution to obtain the vertical resolution. The gain and the vertical resolution are the output parameters of the routine. When a second call to the routine occurs (i.e., a second smoothing operation occurs), the cut-off width output from the first call is not used anymore. Instead, the gain output from the first call is used as input parameter for the second call, together with the sam-

pling resolution and the coefficients of the second filter. The product of the input gain and gain computed from the second filter is the new gain from which the routine identifies the cut-off frequency. A new vertical resolution is obtained by multiplying the inverse of the newly computed doubled cut-off frequency by the sampling resolution. The new gain and the new vertical resolution are the output parameters of the routine after the second call. The procedure is repeated as many times as needed, i.e., as many times as a smoothing or differentiation operation occurs.

The standardization tools became available in summer 2011. They were distributed to several members of the ISSI team for testing and validation. Using simulated lidar signals and a series of Monte Carlo experiments, their implementation was validated for several NDACC ozone and temperature lidar algorithms. Several examples of this validation are provided in the ISSI team report (Leblanc et al., 2016a). Ideally, an NDACC-wide implementation should follow. The implementation will not be considered complete until the vertical resolution outputs of all contributing data processing software have been quantified and validated following the same procedure as that described in Leblanc et al. (2016a).

5 Summary and discussion

In the present work, we recommended using one or two standardized definitions of vertical resolution that can unequivocally describe the impact of vertical filtering on the ozone and temperature lidar profiles. The coefficients of the filter used in the vertical smoothing operation are chosen by the lidar investigator, and therefore constitute the key information for the derivation of vertical resolution using a standardized definition.

The first standardized definition recommended for use in the NDACC ozone and temperature lidar algorithms is based on the width of the response to a finite-impulse-type perturbation. The response is computed by convolving the filter coefficients with an impulse function, namely, a Kronecker delta function for smoothing filters and a Heaviside step function for derivative filters. Once the response has been computed, the standardized definition of vertical resolution proposed by the ISSI team is given by $\Delta z = \delta z \times H_{\mathrm{FWHM}}$, where δz is the lidar's sampling resolution and H_{FWHM} is the full width at half maximum (FWHM) of the response, measured in sampling intervals. Following this definition, an unsmoothed signal yields the best possible vertical resolution $\Delta z = \delta z$ (one sampling bin). This definition was recommended by the ISSI team because it is already widely used within the NDACC community, and it has many points of commonality with the averaging kernels reported for the retrieval of atmospheric species using optimal estimation methods. This definition also allows multiple smoothing occurrences to be treated analytically in a simple and exact manner.

The other recommended definition relates to digital filtering theory. After applying a Laplace transform to a set of filter coefficients, we can derive the filter transfer function and gain, which characterize the effect of the filter on the signal in the frequency domain. A cut-off frequency value f_{C} can be defined as the frequency at which the gain equals 0.5, and vertical resolution can then be defined by the relation $\Delta z = \delta z/(2 f_{\mathrm{C}})$. Unlike common practice in the field of spectral analysis, a factor $2 f_{\mathrm{C}}$ instead of f_{C} was indeed used here to yield values conveniently close to those obtained with the impulse response definition. The present definition therefore yields vertical resolution values expressed as multiples of sampling intervals rather than multiples of Nyquist intervals, and an unsmoothed signal yields the best possible vertical resolution $\Delta z = \delta z$ (one sampling interval). This result maps to the frequency domain as twice the Nyquist frequency. Like in the impulse response case, the values of vertical resolution computed for multiple, successive smoothing operations are conceptually, theoretically, and numerically exact.

The ISSI team developed numerical tools to support the implementation of these definitions across the NDACC lidar groups. The tools consist of ready-to-use "plug-in" routines written in IDL, FORTRAN, MATLAB, C++, and PYTHON that can be inserted into any lidar data processing software each time a smoothing operation occurs in their data processing chain. The routine's input parameters are the lidar sampling resolution and the coefficients of the smoothing filter locally applied, and the output parameter is the vertical resolution following the impulse-response-based standardized definition or the cut-off frequency-based standardized definition. When multiple smoothing operations occur within the same data processing chain, the plug-in routines must be called each time smoothing occurs, but the final vertical resolution to be reported is computed only at the final occurrence. The values output by the routines after the last call are reported in the lidar data files together with the ozone or temperature profiles. These standardized values of vertical resolution are theoretically and numerically exact, even after multiple filtering occurrences. Using simulated lidar signals and a series of Monte Carlo experiments, their implementation was validated for several NDACC ozone and temperature lidar algorithms. Examples of this validation are provided in the ISSI team report (Leblanc et al., 2016a).

6 Conclusion

Over the years, NDACC lidar PIs have been providing temperature and ozone profiles using a wide range of vertical resolution schemes and values, and these values were reported using different definitions. Here we did not recommend using a specific vertical resolution scheme, but instead we recommended using standardized definitions of vertical resolu-

tion that can be used consistently across lidar observation networks. The proposed approach was designed so that the standardized definitions can be implemented easily and consistently by all lidar investigators (e.g., NDACC, TOLNet). Though the recommendations apply to the retrieval of ozone by the differential absorption technique and temperature by the density integration technique, they can likewise apply to the retrieval of other NDACC species such as water vapor (Raman and differential absorption techniques), temperature (rotational Raman technique), and aerosol backscatter ratio with the exception of the optimal estimation method (OEM) for the retrievals of temperature and water vapor recently proposed by Sica and Haefele (2015, 2016), for which vertical resolution is determined from the FWHM of the OEM's averaging kernels.

In our two companion papers (Leblanc et al., 2016b, c), the ISSI team provided recommendations on the standardized treatment of uncertainty for the NDACC ozone and temperature lidars (Part 2 and Part 3 respectively). It is anticipated that the widespread use of the standardized definitions and approaches proposed in our three companion papers will significantly improve the interpretation of atmospheric measurements, whether these measurements are made for validation purposes (e.g., comparison of correlative measurements) or scientific purposes (e.g., studies of vertical structures observed in the measured profiles).

7 Data availability

The data shown here are not publicly available. However, they can be obtained by contacting the first author at thierry.leblanc@jpl.nasa.gov.

The Supplement related to this article is available online at doi:10.5194/amt-9-4029-2016-supplement.

Acknowledgements. This work was initiated in response to the 2010 call for international teams of experts in earth and space science by the International Space Science Institute (ISSI) in Bern, Switzerland. It could not have been performed without the travel and logistical support of ISSI. Part of the work described in this report was carried out at the Jet Propulsion Laboratory, California Institute of Technology, under agreements with the National Aeronautics and Space Administration. Part of this work was carried out in support of the VALID project. Robert J. Sica would like to acknowledge the support of the Canadian National Sciences and Engineering Research Council for support of the University of Western Ontario lidar work. The team would also like to acknowledge J. Bandoro for his help in the design of the MATLAB filtering tools.

Edited by: H. Maring
Reviewed by: M. J. Newchurch and one anonymous referee

References

Argall, P. S. and Sica, R. J.: A comparison of Rayleigh and sodium lidar temperature climatologies, Ann. Geophys., 25, 27–35, doi:10.5194/angeo-25-27-2007, 2007.

Arshinov, Y. F., Bobrovnikov, S. M., Zuev, V. E., and Mitev, V. M.: Atmospheric-temperature measurements using a pure rotational Raman lidar, Appl. Opt., 22, 2984–2990, 1983.

Beyerle, G. and McDermid, I. S.: Altitude Range Resolution of Differential Absorption Lidar Ozone Profiles, Appl. Opt., 38, 924–927, 1999.

Birge, R. T. and Weinberg, J. W.: Least-Squares' Fitting of Data by Means of Polynomials, Rev. Mod. Phys., 19, 298 pp., 1947.

D'Amico, G., Amodeo, A., Baars, H., Binietoglou, I., Freudenthaler, V., Mattis, I., Wandinger, U., and Pappalardo, G.: EARLINET Single Calculus Chain – overview on methodology and strategy, Atmos. Meas. Tech., 8, 4891–4916, doi:10.5194/amt-8-4891-2015, 2015.

Eisele, H. and Trickl, T.: Improvements of the aerosol algorithm in ozone lidar data processing by use of evolutionary strategies, Appl. Opt., 44, 2638–2651, 2005.

Godin, S., Carswell, A. I., Donovan, D. P., Claude, H., Steinbrecht, W., McDermid, I. S., McGee, T. J., Gross, M. R., Nakane, H., Swart, D. P. J., Bergwerff, H. B., Uchino, O., von der Gathen, P., and Neuber, R.: Ozone Differential Absorption Lidar Algorithm Intercomparison, Appl. Opt., 38, 6225–6236, 1999.

Godin-Beekmann, S., Porteneuve, J., and Garnier, A.: Systematic DIAL lidar monitoring of the stratospheric ozone vertical distribution at Observatoire de Haute-Provence (43.92 degrees N, 5.71 degrees E), J. Environ. Monit., 5, 57–67, doi:10.1039/b205880d, 2003.

Gross, M. R., McGee, T. J., Ferrare, R. A., Singh, U. N., and Kimvilakani, P.: Temperature measurements made with a combined Rayleigh-Mie and Raman lidar, Appl. Opt., 36, 5987–5995, 1997.

Hamming, R. W.: Digital Filters, Third Edition ed., Prentice Hall, Englewood Cliffs, New Jersey, ISBN-10: 0-13-212812-8, 1989.

Hauchecorne, A. and Chanin, M. L.: Density and temperature profiles obtained by lidar between 35-km and 70-km, Geophys. Res. Lett., 7, 565–568, 1980.

Iarlori, M., Madonna, F., Rizi, V., Trickl, T., and Amodeo, A.: Effective resolution concepts for lidar observations, Atmos. Meas. Tech., 8, 5157–5176, doi:10.5194/amt-8-5157-2015, 2015.

Kaiser, J. F. and Reed, W. A.: Data smoothing using low-pass digital-filters, Rev. Sci. Instr., 48, 1447–1457, 1977.

Kempfer, U., Carnuth, W., Lotz, R., and Trickl, T.: A wide-range ultraviolet lidar system for tropospheric ozone measurements: Development and application, Rev. Sci. Instr., 65, 3145–3164, doi:10.1063/1.1144769, 1994.

Leblanc, T., McDermid, I. S., Hauchecorne, A., and Keckhut, P.: Evaluation of optimization of lidar temperature analysis algorithms using simulated data, J. Geophys. Res., 103, 6177–6187, 1998.

Leblanc, T., McDermid, I. S., and Walsh, T. D.: Ground-based water vapor raman lidar measurements up to the upper troposphere and lower stratosphere for long-term monitoring, Atmos. Meas. Tech., 5, 17–36, doi:10.5194/amt-5-17-2012, 2012.

Leblanc, T., Sica R., van Gijsel, J. A. E., Godin-Beekmann, S., Haefele, A., Trickl, T., Payen, G., and Liberti, G.: Standardized definition and reporting of vertical resolution and uncertainty

in the NDACC lidar ozone and temperature algorithms, ISSI Team on NDACC Lidar Algorithms Report, available for download at: http://www.issibern.ch/teams/ndacc/ISSI_Team_Report.htm (last access: 21 August 2016), 2016a.

Leblanc, T., Sica, R. J., van Gijsel, J. A. E., Godin-Beekmann, S., Haefele, A., Trickl, T., Payen, G., and Liberti, G.:Proposed standardized definitions for vertical resolution and uncertainty in the NDACC lidar ozone and temperature algorithms – Part 2: Ozone DIAL uncertainty budget, Atmos. Meas. Tech., 9, 4051–4078, doi:10.5194/amt-9-4051-2016, 2016b.

Leblanc, T., Sica, R. J., van Gijsel, J. A. E., Haefele, A., Payen, G., and Liberti, G.: Proposed standardized definitions for vertical resolution and uncertainty in the NDACC lidar ozone and temperature algorithms – Part 3: Temperature uncertainty budget, Atmos. Meas. Tech., 9, 4079–4101, doi:10.5194/amt-9-4079-2016, 2016c.

Mégie, G., Allain, J. Y., Chanin, M. L., and Blamont, J. E.: Vertical Profile of Stratospheric Ozone by Lidar Sounding from Ground, Nature, 270, 329–331, 1977.

Rabiner, L. R. and Gold, B.: Theory and Application of Digital Signal Processing, Prentice-Hall, Inc., Englewood Cliffs, N.J., 126–127, doi:10.1002/piuz.19760070413, 1975.

Savitzky, A. and Golay, M. J. E.: Smoothing and differentiation of data by simplified least squares procedures, Anal. Chem., 36, 1627–1639, 1964.

Sica, R. J. and Haefele, A.: Retrieval of temperature from a multiple-channel Rayleigh-scatter lidar using an optimal estimation method, Appl. Opt., 54, 1872–1889, doi:10.1364/ao.54.001872, 2015.

Sica, R. J. and Haefele, A.: Retrieval of water vapor mixing ratio from a multiple channel Raman-scatter lidar using an optimal estimation method, Appl. Opt., 55, 763–777, doi:10.1364/ao.55.000763, 2016.

Sica, R. J. and Russell, A. T.: Measurements of the effects of gravity waves in the middle atmosphere using parametric models of density fluctuations. Part I: Vertical wavenumber and temporal spectra, J. Atmos. Sci., 56, 1308–1329, 1999.

Steinier, J., Termonia, Y., and Deltour, J.: Smoothing and differentiation of data by simplified least square procedure, Anal. Chem., 44, 1906–1909, doi:10.1021/ac60319a045, 1972.

Swart, D. P. J., Apituley, A., Spakman, J., Visser, E. P., and Bergwerff, H. B.: RIVMs tropospheric and stratospheric ozone lidars for European and global monitoring networks, Proceedings of the 17th International Laser Radar Conference, Laser Radar Society of Japan, Sendaï, Japan, 1994, 405–408, 1994.

Trickl, T.: Tropospheric trace-gas measurements with the differential-absorption lidar technique, in: Recent Advances in Atmospheric Lidars, L. Fiorani, V. Mitev, Eds., INOE Publishing House, Bucharest (Romania), Series on Optoelectronic Materials and Devices, Vol. 7, ISSN: 1584-5508, ISSN: 978-973-88109-6-9, 87–147, revised version available at: http://www.trickl.de/DIAL.PDF (last access: 21 August 2016), 2010.

VDI: Remote sensing – Atmospheric measurements with LIDAR – Measuring gaseous air pollution with DAS LIDAR, Guideline 4210, Technical rule, Verein Deutscher Ingenieure, Beuth, Düsseldorf, Germany, 1–52, 1999 (in German).